Journal of the Australian Ceramic Society
https://doi.org/10.1007/s41779-018-00292-5

RESEARCH

In vivo studies of titanium implant surface treatment by sandblasted, acid-etched and further anchored with ceramic of tetracalcium phosphate on osseointegration

Jian-Chih Chen[1,2] · Chia-Ling Ko[3,4,5] · Dan-Jae Lin[6,7] · Hui-Yu Wu[3,4] · Chun-Cheng Hung[4,8] · Wen-Cheng Chen[3,4,6]

Received: 15 August 2018 / Revised: 22 October 2018 / Accepted: 13 December 2018

Abstract

The objective was to investigate and compare the osseointegrative responses of sandblasted/acid-etched (SLA) and calcium phosphate (CaP) implants in vivo. The CaP implant was prepared by control group of SLA surface modification and anchoring with sintering ceramic of tetracalcium phosphate (TTCP) to form a mechanical interlocking film. Customized screw Ti implants (size Ø 2.0 mm × 6 mm length) were utilized to histologically examine the bone-to-implant contact (BIC) after implantation. The implant stability quotient scales in the postoperative implants within femurs were recorded. Subsequently, the postoperative implants were scanned using microcomputed tomography (micro-CT), and the topography was examined microscopically to analyze the BIC conditions. The SLA and CaP implant groups showed increased bone mineral density (g/cm^3) and BIC (%). Compared with the SLA implant, the CaP implant with TTCP improved the early osteointegration of the BIC at 1-month post-operation and demonstrated quantitative effects on the BIC at 1-month post-operation. SLA and CaP implants all showed good osseointegration through micro-CT analysis (1–6 months). The current findings suggest the CaP anchoring Ti surface demonstrated improvement in early stages of osseointegration and thus shows the potential clinical benefits of TTCP anchoring on Ti surfaces in bone-level solutions.

Keywords Titanium · Calcium phosphate · Surface modification · Sandblasted and acid etched (SLA) · Histological

Introduction

In the past decade, surface innovation in osseointegrated implants focused on topographic and physiochemical changes [1]. Well-designed implants are utilized not only to modify the geometry of implants but also to change the chemical properties of their surfaces. Different surface characteristics, such as surface chemical compositions, morphologies,

Chun-Cheng Hung has equal contribution to correspondence

Electronic supplementary material The online version of this article (https://doi.org/10.1007/s41779-018-00292-5) contains supplementary material, which is available to authorized users.

✉ Wen-Cheng Chen
wencchen@fcu.edu.tw; wincheng0925@yahoo.com.tw

[1] Department of Orthopedics, Faculty of Medical School, College of Medicine, Kaohsiung Medical University, Kaohsiung 807, Taiwan

[2] Department of Orthopaedics, Kaohsiung Municipal Siaogang Hospital, Kaohsiung 812, Taiwan

[3] Department of Fiber and Composite Materials, Feng Chia University, 100, Wenhwa Rd., Seatwen, Taichung 407 40724, Taiwan, Republic of China

[4] Dental Medical Devices and Materials Research Center, College of Dental Medicine, Kaohsiung Medical University, Kaohsiung 807, Taiwan

[5] Laser and Additive Manufacturing Technology Center, Industrial Technology Research Institute, Hsinchu 310, Taiwan

[6] Department of Dental Hygiene, China Medical University, Taichung 404, Taiwan

[7] School of Dentistry, College of Medicine, China Medical University, Taichung 404, Taiwan

[8] Department of Prosthodontics, Kaohsiung Medical University Hospital, Kaohsiung 807, Taiwan

Published online: 05 January 2019

topography, roughness, and wettability, play important roles during the early healing of the bone that is integrated to the implant after operation [2–7].

Numerous surface modifications, such as grit blasting, acid etching [8, 9], Ti or Ti/calcium phosphates (CaPs) combined spraying techniques, and CaP coating by plasma, laser, or anodization, have been applied to fabricate different Ti implant surfaces [10]. Most of these surfaces are commercially available and exhibit proven clinical efficacy (> 95% over 5 years) [3]. Osteoconductive CaP coatings promote bone healing and apposition, which lead to the rapid biological fixation of implants. Calcium ion doping is generally combined with high-energy plasma, laser deposition, or electrical oxidation (e.g., applying micro-arc oxidation methods on the topography of dental implants) [11].

CaPs are important compounds in many fields, such as in geology, chemistry, biology, and medicine, and play an important role in the design and development of medical devices. The recognition of tetracalcium phosphate (TTCP) is the hardness and durability when compared to the other CaPs. The structural formula of TTCP is $Ca_4(PO_4)_2O$. Thus, TTCP leads to the most basic CaPs and exhibits a high atomic Ca/P ratio of 2.0, making TTCP the most calcium-abundant phosphate when TTCP is dissolved in an aqueous solution. Besides, the biodegradability decreases following the sequence: TTCP < hydroxyapatite (HA) < β-TCP (tricalcium phosphate) < α-TCP) due to the phases possess the same tendency of solubility. Our previous in vitro study results suggest that sandblasting and acid etching (SLA) followed by physically anchoring TTCPs on implant surfaces can accelerate progenitor bone cell mineralization [12]. The designed Ti implants were prepared for rabbit femur portions using our innovative TTCP grit anchoring technique in vivo in this study. Measurement of the implant stability quotient (ISQ) through resonance frequency analysis (RFA), microcomputed tomography (micro-CT) scanner analysis, and histological and histomorphometric analyses were performed.

Materials and methods

Preparation of Ti implants

Sixteen commercially pure, grade IV, cylindrical Ti (ASTM 67) implants treated with SLA and CaP anchorage with 74% anchoring rate were prepared. For integration tests, the not regular mini-implants of the commercial Ti were machined and initially cut at 2 mm (outer diameter) × 6 mm (length) by a computer numerical control (CNC) machine (Fig. 1). The samples then underwent SLA [12]. The polished surfaces of the implants were first sandblasted with alumina (Al_2O_3) particles 150–250 μm in size by utilizing an air compressor. The samples were then acid etched to fabricate surfaces for the SLA group. The etching solution contained HCl (37%), H_2SO_4 (96%), and H_2O at a volume ratio of 1:1:1. All specimens were washed, dried, and further sandblasted with TTCP (CaP group). The CaP specimens were sandblasted with TTCP particles (10.1 ± 0.7 μm) by utilizing an air compressor with 4–6 kg/m^2 powder that was blasted over a 3-cm distance for 10 s [12].

Surface characterization

The CaP implant was embedded in the epoxy resin and then sectioned into two parts for grinding and polishing to analyze the physically anchored thickness of TTCP. The anchored profile of the CaP group was studied through its cross-sectional images obtained via scanning electron microscopy (SEM, Hitachi S-3000N, Japan) coupled with energy-dispersive spectroscopy (Horiba EX220, Japan).

In vivo testing

The animal testing procedures employed in this study were approved by the Institutional Animal Care and Use Committee of Kaohsiung Medical University. National Institutes of Health (NIH) guidelines for the care and use of laboratory animals (NIH Publication #85-23 Rev. 1985) were observed. A total of 16 rabbits were randomly divided into four groups with implantation periods of 1, 2, 3, and 6 months. The SLA and CaP groups were implanted in the right and left femurs, respectively. The rabbits were terminated 1, 2, 3, and 6 months after surgery, and the femur portions were immediately excised. The femurs were scanned at 35-mm intervals at 89 kV and 100 mA by micro-CT scanner analysis (SkyScan1076; SkyScan, Kontich, Belgium). The trabecular bone structure parameters that were measured for the specific regions of femurs in vivo are listed in supplementary (Table S1). ISQ (Osstell, Gothenburg, Sweden) was also accessed using RFA before tissue fixation ($n = 3$). The retrieved implants with bone tissues were fixed with formalin for non-decalcified plastic embedding. The sectioned implants with bones were thinned out to a final thickness of 1 mm to observe the bone contact interface condition of the implants through SEM. The sectioned slices were further thinned out to a final thickness of 100 μm, polished, and glued to slides with Permount (Fisher Scientific, Fair Lawn, NJ). These sections were stained with hematoxylin-eosin. The slides were histologically examined under an optical microscope, and a digital image analysis software was used to calculate the bone-to-implant contact (BIC) ratio for histomorphometrical measurements. Two slides from the mid-portion of each implant were used for histologic and histomorphometric evaluation. The evaluation was performed single blinded. Two independent persons performed the histomorphometrical analyses to ensure that no significant differences occurred between the

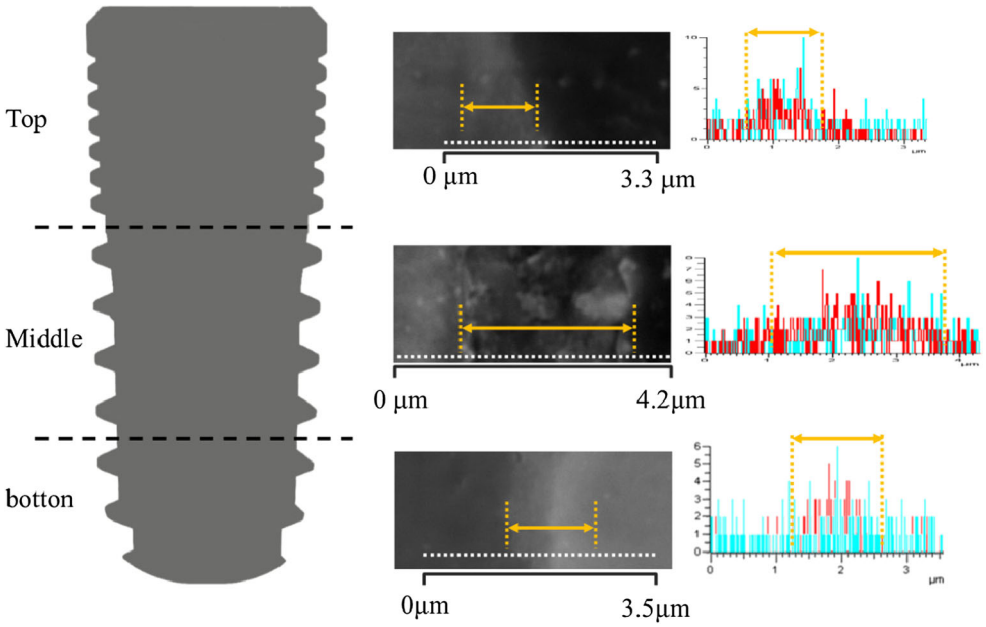

Fig. 1 Customized implant design. Lateral view of the designed implant (6 mm length, 2 mm diameter). CaP anchorage depth distribution was assessed by elemental scanning lines of Ca (red line) and P (blue line) on the constructed geometry on the Ti implant surfaces

investigators and the mean values of quantitative measurement performed ($n = 4$).

Results

Surface characteristics

All implants exhibited the same dimensional shapes and were subjected to the same submerged procedures, although the surface modifications of SLA and CaP were different (Fig. 1). The depth of the capping particles on the implant was carefully controlled to ensure that the surface being treated utilized the same anchored power and energy. However, variations in the TTCP capping rate still existed (Fig. 1). The largest anchored thickness at the middle of the implant geometry was estimated to be 3 μm, and the top and bottom sides of the implant were grossly estimated to be < 3 μm.

In vivo results of X-ray, 3D micro-CT, implant stability, elemental mapping, and histological analysis

All implants that were inserted in the rabbit femurs were included, and these conditions indicated that no implant failed during the measurements. The two groups of implants were maintained at stable ISQ values in vivo throughout the 3 months post-operation (Fig. 2). Moreover, the initial stability of both groups gradually increased and reached the plateau at 2 months post-operation due to the difference observed was not statically significant between the groups in ISQ values of SLA and CaP at third month of post-implantation, indicating that low mechanical stability was still being enforced by the bone remodeling process (osseointegration).

X-ray and 3D micro-CT results indicated that the interfaces of the implants and surrounding tissues showed no cracks and evident voids (Fig. 3).

The 3D micro-CT databases were analyzed and compared with the known density of bone tissues. Except for the 1 month of post-operation, the BMD indexes of the modified CaP implant were all slightly higher than those of the SLA implant at 6 months (Fig. 4) but analysis showed no significance between means ($p > 0.05$).

The micro-CT images showed that the SLA and CaP implants differed in osseointegration at 2 and 6 months post-operation. SEM and line-scanned elemental mapping also confirmed that the bone junction interfaces with implants were

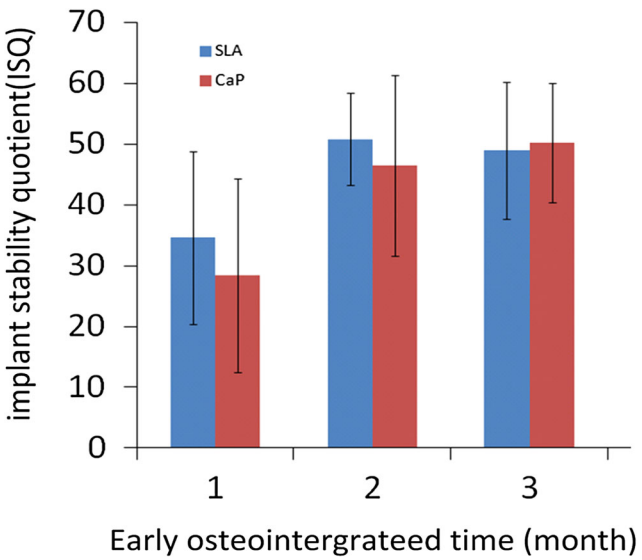

Fig. 2 Implant stability quotient values of an SLA and modified CaP implant at 1, 2, and 3 months post-operation ($n = 3$)

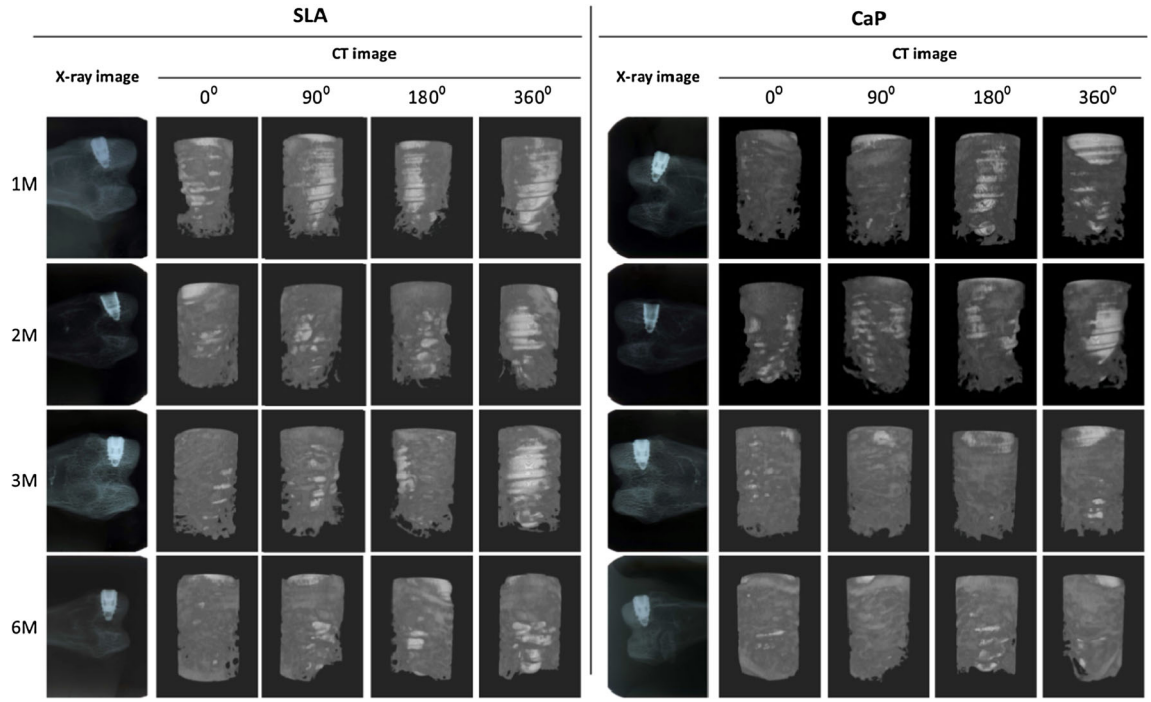

Fig. 3 X-ray images and the four rotating images of high-power 3D micro-CT view. Left: Ti group through SLA surface modification. Right: CaP group of the SLA surface with TTCP further anchored

in close contact with the implant surfaces but still exhibited clear boundaries even at 2 months post-operation (Fig. 5). However, the implant surroundings at 6 months post-operation were fully dense and bound to the bone without any gaps, particularly in the CaP group. This result is consistent with the elemental line-scanning results on the bone and implant interfaces (Fig. 5).

The light image examinations at 6 months are shown in Figs. 6 and 7a. Comparative histological images for each surface were used to analyze the bones along the line passing through the coronal part to the implant apex [2, 9]. The lamellar bone content increased from 2 to 6 months of osseointegration. The observed results of BIC percentage increased with time at 2 months post-operation and the difference within the CaP and SLA groups was statistically significant ($p < 0.05$) (Fig. 7b). The phenomenon of BIC percentage gradually increased with time; however, a slight decreased was observed after 6 months of post-implantation. The difference between time groups at third and sixth months of post-implantation in BIC percentage was not statistically significant ($p > 0.05$).

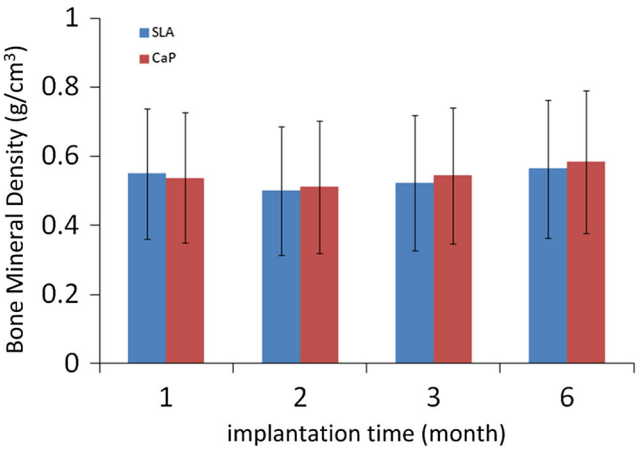

Fig. 4 Quantitate analysis of bone mineral density from the micro-CT database ($n = 4$, $p > 0.05$) (detailed data of bone-specific surface (BS/BV), bone surface density (BS/TV), and bone volume versus total volume (BV/TV) are provided in the supplementary material)

Discussion

The TTCP-anchored thicknesses were estimated to range from 12.6 to 18.3 μm, which is consistent with our previous study on TTCP anchorage through a standardized flat plate [12]. However, from the implant surface observations in this study (Fig. 1), the customized mini-implant showed variations in the TTCP-anchored thickness due to the effects of screw thread geometry, face angle, thread pitch, thread depth, and thickness or helix angle. Due to the differences in spray distance caused by the shape effect of the mini-implant in this study, the results of the actual implant test conditions are also different from those of the standard flat test specimens. Implant stability was measured after the femur was removed, and the ISQ differences between the two groups were measured. Three main factors affected the ISQ values: (1) the strength and stiffness of implants, such as geometric design (e.g., the surface

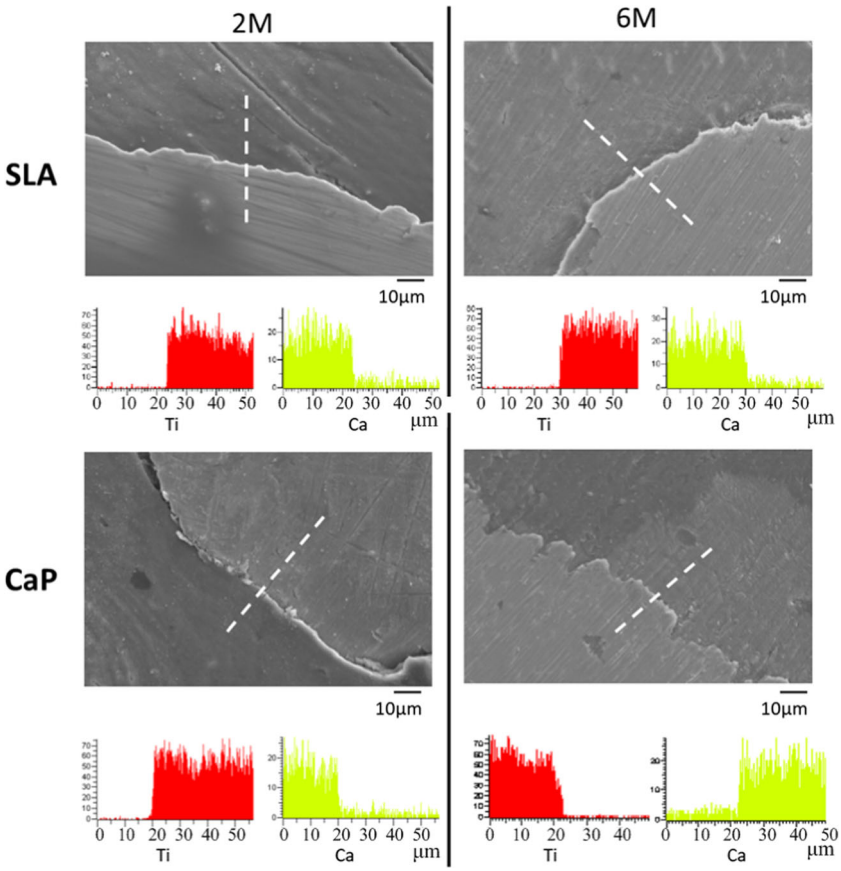

Fig. 5 Results of the line-scanned elemental mapping of the SLA and CaP group interfaces at 2 and 6 months post-operation. The line-scanned results show that these groups are always in close contact with the implant surface and with no gaps at the interfaces regardless of implant time courses

components after special treatment or electronic doping); (2) the implant sites of the bone tissue, cortical bone, and cancellous bone that comprised the bone density ratio; and (3) the bonding strength between the bone and implant interfaces [13–16]. The implant that we used was customized with the smallest geometric size (size Ø 2.0 mm × 6 mm length) relative to other mini-implants [13]. The normal implant stability quotient (ISQ) scales of implants used for clinical application are > 60 to exhibit initial stability. However, the measured ISQ values were < 60, specifically 53.3 (IQR 8.3) and 60.5 (IQR

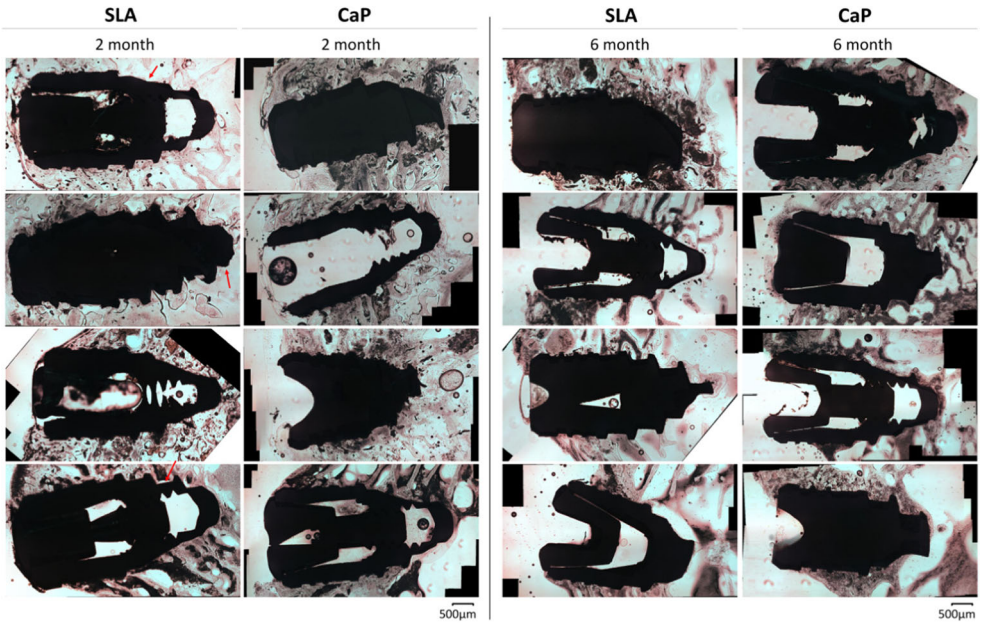

Fig. 6 Optical scope micrographs of the non-decalcified tissue slice that show the interfaces between the implants and bone tissues through the surface modification of the SLA and CaP condition refraction at 2 and 6 months post-operation. The red arrows show that the morphological integration is strong for bones

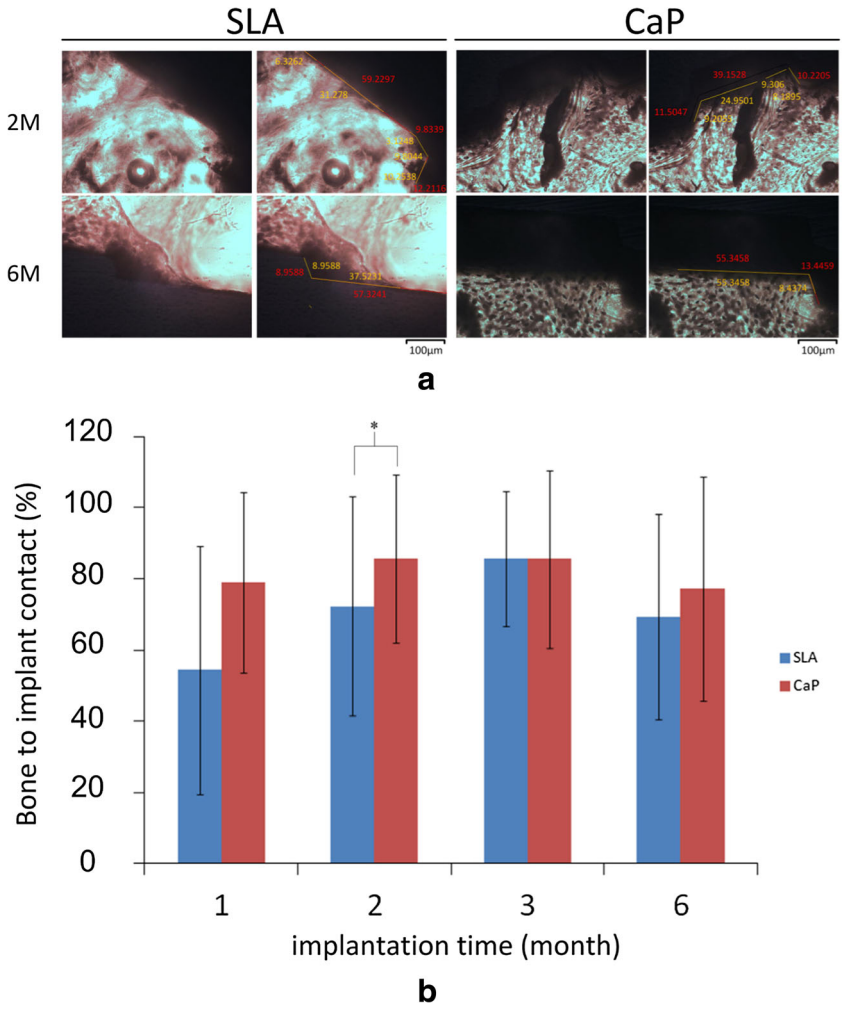

Fig. 7 Histological light micrographs of the non-calcified tissue by 6 months post-operation. **a** Histological observation and histomorphometry regenerated bone minerals are indicated in yellow lines. Voids are indicated in red lines. **b** Respective BIC (%) measured (*$p < 0.05$)

5.5) for the 3M™ESPE™MDIs (Ø 1.8 mm × 10 mm) and 58.5 (IQR 4.75) and 65.5 (IQR 9.3) for the Ankylos® (Ø 3.5 mm × 8 mm) implants at 6 weeks post-operation. Geometrical mini-implants with ISQ results that were comparable to those demonstrated in this study were difficult to find in literature. The favorable short-term results for our customized mini-implants with SLA and a modified CaP surface after 4 weeks of healing exhibited > 30 ISQ in general. The ISQ values still increased until a plateau was reached at > 50 after 8 weeks (Fig. 2). This finding reflects good and continuous bone integration without decay.

The 3D micro-CT analysis presented in Fig. 3 shows the osteointegration occurring in the surroundings between the interfaces of the bone tissue and implant images, and each osseointegration side can be reached by installing implants after the SLA and CaP surface treatments. The complete CT scan data are presented in the uploaded Supplementary material. The differences in the osseointegration qualities from the 3D micro-CT view of the light gray images can be directly observed at 1, 2, and 3 months post-operation (Figs. 2 and 3 and in the Supplementary material). The entire implant surface was completely generated and surrounded the bone tissues of the CaP group, whereas the SLA group did not exhibit similar conditions. No statistically significant difference in micro-CT quantized measurements was found between the SLA and CaP groups (Fig. 4). At 6 months after implantation, the two groups exhibited regenerated bone tissues on the Ti implant surface because the bone tissues almost covered the entire implant, and the light gray surface of the original implants cannot be directly observed. Raw observations of the SLA and CaP groups through the images and elemental mapping further confirmed that these implant cases generated a suitable level of osseointegration after 6 months of implantation (Fig. 5). Large portions of the bone tissue were also generated and maintained the bone level in the CaP group, especially at 2 months post-operation (Figs. 2 and 5). Notably, newly formed bones extended from the cortical zone to the apex zone of the implant (Fig. 6).

The implant success rate was largely related to the early implant integration [9, 16–19], and the BIC of the CaP implant was higher than that of the SLA implant at 1 month post-operation. The BIC slightly decreased at 6 months post-

operation (Fig. 7b). Bone mineral analyses, such as ISQ and BMD (Figs. 2 and 4 and in the Supplementary material), exhibited the same trend despite the slight variation. The detailed histological results also showed that both groups of modified surfaces on Ti failed to detect any fibrous tissue that surrounds the implant area at the same implantation time (Fig. 7a).

The combination of organic and inorganic constituents is a major mechanism for consequent functionality and biological efficacy, which allows bone regeneration [20–22]. The present study introduced an implant surface treatment method with integrated tissues, where Ca^{2+} ions are provided to advance the growth of bone cells. The solubility phase diagram shows that the TTCP with a Ca-to-P ratio of 2.0 easily dissolves in acidic environments because the pH of the implantation site is acidic in the acute inflammation stage [23], releasing a large quantity of Ca^{2+} ions and phosphate (PO_4^{3-}) ion. Ca^{2+} ions demonstrate a high affinity for TiO_2 and are absorbed on the oxide layer of implant surfaces. Researchers suggest that proteins are primarily absorbed on an implant surface through Ca^{2+} ions [1]. The Ca^{2+} can be bound to many polyanions of proteoglycans, which play a key role in binding bone cells, and glycosaminoglycan binds covalently to the protein ore of proteoglycans [24]. Osteoblasts are responsible for the mineralization of the osteoid matrix, promote pH higher than 8.5 by excretion of ammonia [25]. That leads the ion exchanges and interactions of Ca^{2+} and PO_4^{3-} with biological environment will facilitate the osseointegration. The current study demonstrated that a clear relation exists between the surface modifications in SLA. On the basis of the measurements in this study, further anchorage with CaP increases the bone mineral rate with the maturation of bone tissue during healing.

Conclusion

Both implants reached the healing and bone formation rates at osteoregeneration periods of 1, 2, 3, and 6 months. No gaps within their respective interfaces were grossly observed. However, comprehensive in vivo evaluation revealed that the osseointegration performance of the SLA with anchored CaP on the implant surface was better than that of the SLA-only group in contact with the implant percentage at 1-month post-operation. The results of micro-CT measurements and histological analysis revealed improved healing trends and better bone-maintained level in the CaP implant group than in the SLA implant group at an earlier stage. New bone around the CaP implants can be regenerated and shorten the time required for osseointegration.

Acknowledgements The authors acknowledge and appreciate the assistance of Ms. Cian-Hua Liou, Ms. Ya-Yuan Chang, and Present Company Tuo-Huo Chang who customized and free provided the screw implants by Alliance Global Technology Co. in this research. The authors also thank the Precision Instrument Support Center of Feng Chia University, which provided the fabrication and measurement facilities. The assistance of the participants in this research is also acknowledged.

Funding This work was supported by the Ministry of Science and Technology, Taiwan [grant numbers MOST 103-2221-E-035-099- and 105-2221-E-035-021-MY3].

Compliance with ethical standards

The animal testing procedures employed in this study were approved by the Institutional Animal Care and Use Committee of Kaohsiung Medical University. National Institutes of Health (NIH) guidelines for the care and use of laboratory animals (NIH Publication #85-23 Rev. 1985) were observed.

Conflict of interest The authors declare that they have no conflict of interest.

References

1. Sul, Y.T., Byon, E.S., Jeong, Y.: Biomechanical measurements of calcium-incorporated oxidized implants in rabbit bone: effect of calcium surface chemistry of a novel implant. Clin Implant Dent Relat Res. **6**, 101–110 (2014)
2. Gotfredsen, K., Berglundh, T., Lindhe, J.: Anchorage of titanium implants with different surface characteristics: an experimental study in rabbits. Clin Implant Dent Relat Res. **2**, 120–128 (2000)
3. Le Guéhennec, L., Soueidan, A., Layrolle, P., Amouriq, Y.: Surface treatments of titanium dental implants for rapid osseointegration. Dent Mater. **23**, 844–854 (2007)
4. Buser, D.: Titanium for dental applications (II): implants with roughened surfaces. In: Brunette, D.M., Tengvall, P., Textor, M., Thomsen, P. (eds.) Titanium in Medicine, pp. 876–888. Springer, Berlin (2001)
5. Albrektsson, T., Wennerberg, A.: Oral implant surfaces: part 2-review focusing on clinical knowledge of different surfaces. Int J Prosthodont. **17**, 544–564 (2004)
6. Esposito, M., Coulthard, P., Thomsen, P., Worthington, H.V.: The role of implant surface modifications, shape and material on the success of osseointegrated dental implants, a Cochrane systematic review. Eur J Prosthodont Restor Dent. **13**, 15–31 (2005)
7. Puleo, D.A., Thomas, M.V.: Implant surfaces. Dent Clin N Am. **50**, 323–338 (2006)
8. Teng, F.Y., Ko, C.L., Kuo, H.N., Hu, J.J., Lin, J.H., Lou, C.W., Hung, C.C., Wang, Y.L., Cheng, C.Y., Chen, W.C.: A comparison of epithelial cells, fibroblasts, and osteoblasts in dental implant titanium topographies. Bioinorg Chem Appl. **2012**, 687–692 (2012)
9. Calvo-Guirado, J.L., Satorres-Nieto, M., Aguilar-Salvatierra, A., Delgado-Ruiz, R.A., Maté-Sánchez de Val, J.E., Gargallo-Albiol, J., Gomez-Moreno, G., Romanos, G.: Influence of surface treatment on osseointegration of dental implants: histological, histomorphometric and radiological analysis in vivo. Clin Oral Investig. **19**, 509–517 (2015)
10. De Groot, K., Wolke, J.G.C., Jansen, J.A.: Calcium phosphate coatings for medical implants. Proc Inst Mech Eng Part H. **212**, 137–147 (1998)

11. Wennerberg, A., Albrektsson, T.: Effects of titanium surface topography on bone integration: a systematic review. Clin Oral Implants Res. **20**, 172–184 (2009)
12. Ko, C.L., Chang, Y.Y., Liou, C.H., Chen, W.C.: Characterization of the aspects of osteoprogenitor cell interactions with physical tetracalcium phosphate anchorage on titanium implant surfaces. Mater Sci Eng C. **49**, 7–13 (2015)
13. Dhaliwal, J.S., Albuquerque Jr., R.F., Murshed, M., Feine, J.S.: Osseointegration of standard and mini dental implants: a histomorphometric comparison. Int J Implant Dent. **3**, 15 (2017)
14. Sennerby, L., Meredith, N.: Implant stability measurements using resonance frequency analysis: biological and biomechanical aspects and clinical implications. Periodontol. **47**, 51–66 (2008)
15. Scarano, A., Degidi, M., Lezzi, G., Petrone, G., Piattelli, A.: Correlation between implant stability quotient and bone-implant contact: a retrospective histological and histomorphometrical study of seven titanium implants retrieved from humans. Clin Implant Dent Relat Res. **8**, 218–222 (2006)
16. Glauser, R., Lundgren, A.K., Gottlow, J., Sennerby, L., Portmann, M., Petra, R., Hammerle, C.H.F.: Immediate occlusal loading of Brånemark TiUniteTM implants placed predominantly in soft bone: 1-year results of a prospective clinical study. Clin Implant Dent Relat Res. **5**, 47–56 (2003)
17. Fernandes, E.L., Unikowski, I.L., Teixeira, E.R., da Costa, N.P., Shinkai, R.S.: Primary stability of turned and acid-etched screw-type implants: a removal torque and histomorphometric study in rabbits. Int J Oral Maxillofac Implants. **22**, 886–892 (2007)
18. Faeda, R.S., Spin-Neto, R., Marcantonio, E., Guastaldi, A.C., Marcantonio Jr., E.: Laser ablation in titanium implants followed by biomimetic hydroxyapatite coating: histomorphometric study in rabbits. Microsc Res Tech. **75**, 940–948 (2012)
19. Surmenev, R.A., Surmeneva, M.A., Ivanova, A.A.: Significance of calcium phosphate coatings for the enhancement of new bone osteogenesis—a review. Acta Biomater. **10**, 557–579 (2014)
20. Lohmann, C.H., Tandy, E.M., Sylvia, V.L., Hell-Vocke, A.K., Cochran, D.L., Dean, D.D., Boyan, B.D., Schwartz, Z.: Response of normal female human osteoblasts (NHOst) to 17β-estradiol is modulated by implant surface morphology. J Biomed Mater Res Part A. **62**, 204–213 (2002)
21. de Jonge, L.T., Leeuwenburgh, S.C.G., Wolke, J.G.C., Jansen, J.A.: Organicinorganic surface modifications for titanium implant surfaces. Pharm Res. **25**, 2357–2369 (2008)
22. Xie, C., Lu, H., Li, W., Chen, F.M., Zhao, Y.M.: The use of calcium phosphate-based biomaterials in implant dentistry. J Mater Sci Mater Med. **23**, 853–862 (2012)
23. Bigi, A., Boanini, E., Bracci, B., Facchini, A., Panzavolta, S., Segattib, F., Sturba, L.: Nanocrystalline hydroxyapatite coatings on titanium: a new fast biomimetic method. Biomaterials. **26**, 4085–4089 (2005)
24. Ko, C.L., Chen, J.C., Tien, Y.C., Hung, C.C., Wang, J.C., Chen, W.C.: Osteoregenerative capacities of dicalcium phosphate-rich calcium phosphate bone cement. J Biomed Mater Res Part A. **103**, 203–210 (2015)
25. Canilias, M., Pena, P., de Aza, A.H., Rodríguez, M.A.: Calcium phosphates for biomedical applications. Boletín De La Sociedad Española De Cerámica Y Vidrio. **56**, 91–112 (2017)